Original scientific paper

Simultaneous phosphates and nitrates removal from waste-waters by electrochemical process: Techno-economical assessment through response surface methodology

Judicaël Ano[1,✉], Bi G. H. Briton[1], Alain S. Assémian[2], Patrick Drogui[3], Kouassi B. Yao[1] and Kopoin Adouby[1]

[1]*Laboratoire des Procédés Industriels de Synthèse, de l'Environnement et des Energies Nouvelles (LAPISEN), Institut National Polytechnique Félix Houphouët-Boigny, BP 1093, Yamoussoukro, Côte d'Ivoire*

[2]*Laboratoire de Thermodynamique et de Physico-chimie du Milieu (LTPCM), UFR-SFA, Université Nangui-Abrogoua, 02 BP 801 Abidjan 01, Côte d'Ivoire*

[3]*Institut National de la Recherche Scientifique (INRS Eau Terre et Environnement), Université du Québec, 490 rue de la Couronne, Québec City, Canada*

Corresponding author: ✉anojudicael@gmail.com; Tel. +225 0707726310 / 0102605946

Abstract

In this study, a new multiobjective optimization of the simultaneous removal of phosphates and nitrates by electrocoagulation was studied using the Box-Behnken design. Ten aluminium electrodes, connected in a monopolar configuration in a batch reactor, were immersed in synthetic wastewater and then in real wastewater. The optimal conditions and the effects of parameters (current intensity, electrolysis time and initial pH) on phosphate and nitrate removal, the formation of by-products, and the operating cost were assessed in the case of synthetic wastewater. This optimization allowed to eliminate 89.21 % of phosphates, 69.06 % of nitrates with an operating cost of 3.44 USD m^{-3} against 13.67 mg L^{-1} of ammonium generated. Optimal conditions applied to real domestic wastewater made it possible to remove 93 % of phosphates and 90.3 % of nitrates with an ammonium residual of 30.9 mg L^{-1}. The addition of sodium chloride reduced the residual ammonium content to 2.95 mg L^{-1}. Further, XRD analysis of the sludge showed poor crystal structure and the FTIR spectrum suggested that the phosphate is removed by adsorption and co-precipitation.

Keywords
Electrocoagulation; monopolar configuration; phosphates; nitrates; optimization

Introduction

Eutrophication is one of the serious environmental problems worldwide. According to statistics from the Water Research Commission (WRC), South Africa, 54, 53, 48 and 28 % of the lakes in Asia,

Europe, North America and Africa face eutrophication problems, respectively [1]. Manifested by excessive growth of algae on the water bodies due to excess of phosphates and nitrate [2], this phenomenon affects the quality, durability, biodiversity and organoleptic characteristics (colour, taste and odour) of surface water, great reserves for the production of drinking water. The natural evolution of eutrophication in waters is slow but has been accelerated under human intervention in recent decades [3]. This is due to domestic and industrial activities as well as intensive use of fertilisers [2]. The important quantities of effluents produced are beyond the self-purifying capacity of the environment [4], leading to an increase in these nutrients in surface and ground waters. In addition to environmental problems, a high nitrate concentration in drinking water constitutes a health risk, the effects of which are mainly summarised in the synthesis of carcinogenic nitrosamines and the formation of methaemoglobin in infants and pregnant women [5].

To avoid these problems, wastewater must be treated respecting the discharge standards recommended by national and international organizations. Several methods have already been developed and classified into physicochemical processes (ion exchange, membrane technologies, adsorption, chemical precipitation) and biological processes [6,7]. All these methods often have their own limitations in their implementation. Ion exchange, adsorption and membrane techniques do not destroy pollutants but concentrate them in a secondary waste [8]. Chemical precipitation and chemical coagulation require high chemical costs and produce a large amount of sludge [9]. Biological method is slow and requires the removal of biomass sludge and disinfection of the treated water [8]. In addition, this process is very sensitive to several parameters such as temperature, pH, conductivity and toxic compounds [10].

Given the limitations of previous processes, research efforts have led to the development of more efficient electrochemical techniques, such as electroreduction (ER) and electrocoagulation (EC) [11,12]. These methods have many advantages in terms of simplicity of equipment, ease of automation, removal efficiency and use of fewer chemicals [13]. ER is a selective method that applies specifically to certain pollutants such as nitrates and requires often very expensive electrodes (Ti, Pd, Pd/Sn, Ti/IrO$_2$-Pt, *etc.*). However, EC requires cheaper and easily accessible electrodes (Fe and Al) and combines the advantages of several depollution processes such as coagulation-flocculation, flotation and electrooxidation/reduction [9]. This makes it effective in the treatment of a wide variety of pollutants (inorganic or organic) [9]. Unlike chemical coagulation, the EC process involves *in situ* generation of coagulants by electrodissolution of Al or Fe anodes immersed in the effluent following the passage of electric current [14,15]. Simultaneously, water molecules are reduced at the cathode, producing hydroxide ions and hydrogen gas [16,17]. With Al electrodes, the main reactions that take place in the vicinity of the electrodes are expressed by Eqs. (1) and (2) [18-20]:

$$Al \rightarrow Al^{3+} + 3e^- \qquad (1)$$

$$2H_2O + 2e^- \rightarrow H_2 + 2OH^- \qquad (2)$$

Metal cations (Al^{3+}) react spontaneously with hydroxide ions (OH$^-$) to form several coagulant species, including Al(OH)$^{2+}$, Al(OH)$_2^+$, Al(OH)$_3$(insoluble), Al(OH)$_4^-$, Al$_2$(OH)$_2^{4+}$, Al$_6$(OH)$_{15}^{3+}$, Al$_7$(OH)$_{17}^{4+}$ and Al$_8$(OH)$_{20}^{4+}$, which are capable of destabilising, coagulating and adsorbing pollutants [19]. Indeed, the insoluble forms of metallic hydroxide Al(OH)$_3$ have large contact surfaces to facilitate the adsorption of pollutants [21].

The removal of phosphates and nitrates taken separately in EC reactor has been reported [20,22-31]. These studies have shown that the effectiveness of treatment is highly dependent on current intensity, electrolysis time and initial effluent pH. A few studies on the simultaneous removal of both phosphate and nitrate have been described in the literature [32]. To the best of our knowledge, the

application of response surface methodology (RSM) for techno-economic assessment of simultaneous phosphate and nitrate removal does not exist in the literature. Moreover, for nitrate EC removal, the removal of its main by-products (ammonium and nitrite) is limited. Ziouvelou *et al.* [33] used a hybrid system (EC/zeolite adsorption) to remove the ammonium generated from water. Benekos *et al.* [34,35] used electrooxidation with anodic electrodes (IrO_2/Ti) as EC post-treatment to remove ammonium generated. The solutions found by these authors are expensive due to the high cost of electrodes and the transfer of ammonium in zeolites that constitute a secondary source of pollution. It would be interesting to find adequate conditions, less expensive, with the EC process and *in situ* production of hypochlorite ions capable of oxidizing ammonium generated into gaseous nitrogen.

The main objective of this study is to optimize the simultaneous removal of phosphate/nitrate in wastewater by the EC process with a minimal content of nitrate by-products. The specific objectives of this work are: i) to model the removal efficiency of nutrients as well as ammonium generated with Box-Behnken design (BBD), ii) to carry out a techno-economic study on the optimal conditions obtained and iii) to apply the optimal conditions on real wastewater.

Experimental

Preparation of domestic synthetic effluent (DSE)

The DSE is a mixture of 100 mg L^{-1} of phosphate and 120 mg L^{-1} of nitrate prepared by simultaneously dissolving 1.5648 g of KNO_3 (Panreac, 99 % purity) and 3.52 g of KH_2PO_4 (Panreac, 99 % purity) in 8 L of distilled water, according to the method described by previous studies [9,25]. The pH of the solutions was measured with a pH meter (HANNA HI 98150) and the initial pH was adjusted using NaOH (1 M) and HCl (1 M) solutions before the beginning of the treatment.

Wastewater phosphate/nitrate -spiking

In view of testing EC in real effluents containing phosphates and nitrates, wastewater samples were collected from the inlet of a treatment plant on the National Polytechnic Institute Félix Houphouët-Boigny campus (Yamoussoukro, in the center of Ivory Cost). The effluent was enriched with phosphate at 100 mg L^{-1} and nitrate at 120 mg L^{-1}. The adjustment of nutrients took into account the initial concentrations of phosphate and nitrate ions in synthetic effluent. The characteristics of effluent are summarized in Table 1.

Table 1 *Characterization of wastewater treatment plant (WTP)*

Physical and chemical parameters	Measured values	Standard
Turbidity, NTU	24.6	25[b]
Conductivity, μS cm^{-1}	807	200-1000[b]
pH	6.93	5.5-8.5[b]
$C_{NO_3^-}$ / mg L^{-1}	120	50[a,c]
$C_{PO_4^{3-}}$ / mg L^{-1}	100	15[b]
$C_{NO_2^-}$ / mg L^{-1}	0.366	3[a]
$C_{NH_4^+}$ / mg L^{-1}	16.6	10[b]
Chemical oxygen demand, mg L^{-1}	110	300[b]

[a]United States environmental protection agency (USEPA)); [b]Standard of Ivorian ministry in charge of environment, water and forest protection; [c]World health organization (WHO)

Electrolytic reactor setup and experimental procedure

The experimental setup consisted of a reactor made of acrylic material (length = width = 12.5 cm; height = 20 cm) and a capacity of 1.7 L. Ten electrodes, flat and rectangular shape (length = 11 cm; width = 10 cm; thickness = 1 mm) each, are vertically immersed in the reactor (immersed area of 110 cm^2) and connected to a direct current generator in the monopolar parallel mode with an inter-electrode distance of 10 mm (Figure 1). The current is imposed by a generator (ELC-AL781D, France) and measured using an ALDA DT-830D ammeter. All EC tests were performed in a batch reactor under a galvanostatic regime. To assure constant homogeneity inside the reactor during EC treatment, the effluent was constantly stirred at 700 rpm [25] with a magnetic stirrer (AGIMATIC -N type).
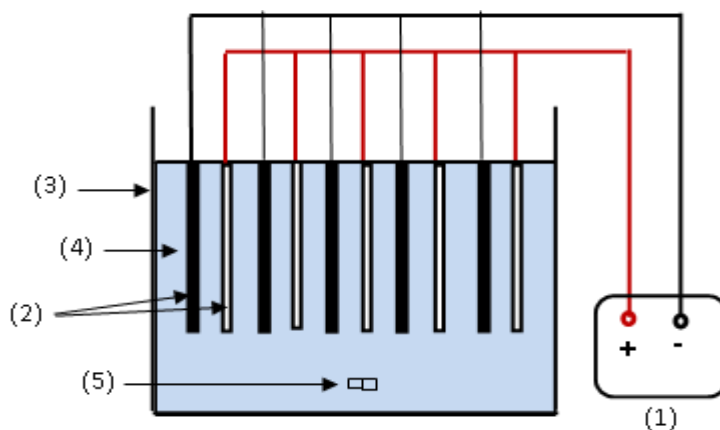

Figure 1. *Schematic representation of EC process setup: (1) current generator; (2) electrodes; (3) electrolytic cell; (4) effluent; (5) magnetic stirrer*

This study was carried out on a domestic synthetic effluent (DSE) in order to optimize the parameters such as current intensity, retention time and initial pH of the effluent. Then, the optimal conditions obtained were applied to a real effluent. The experimental procedure for each EC test is as follows. After having added 2 g of sodium chloride as electrolyte, the treatment of effluent started according to the defined operating conditions. At the end of each test, the content of the reactor was transferred to a 2 L cylinder for 24 hours of settling. Once decanted, the supernatant was filtered under vacuum using a glass microfiber filter Whatman™ (circles diameter 47 mm). The filtrate was collected to determine the residual concentrations of phosphate, nitrate, nitrite and ammonium. The removal efficiency of nutrients (*Y* / %) and the nutrient mass removed (NM$_{removed}$) were calculated using Eqs. (3) and (4) [36]:

$$Y = 100 (C_0 - C_r) / C_0 \tag{3}$$

$$NM_{removed} = (C_0 - C_r) V \tag{4}$$

where C_0 / mg L^{-1}, C_r /mg L^{-1} and *V* /L are the initial nutrient concentration, residual nutrient concentration and volume of the solution, respectively.

Experimental design methodology

The process of phosphate and nitrate removal was described using RSM. Several designs of RSM exist, the best used are the central composite design (CCD) and the Box-Behnken design (BBD). In the framework of this study, BBD was used because it is simple, requiring only three levels in integer values for each factor. In addition, this design requires fewer experiments, so the cost is lower than that of CCD for the same number of factors. The number of experiments (*N*) necessary for the development of the Box-Behnken matrix is defined by Eq. (5):

$$N = 2k\,(k\text{-}1) + N_0 \tag{5}$$

where k is the number of factors and N_0 is the number of tests in the centre of the domain.

According to our previous studies [9,25] the effect of three factors (current intensity (X_1), electrolysis time (X_2) and initial effluent pH (X_3)) on four responses (Y_1: phosphate removal, Y_2: nitrate removal, Y_3: amount of ammonium generated and Y_4: operating cost) was selected in the present study. The three coded values of factors (-1, 0, +1) and the experimental range are shown in Table 2.

__Table 2.__ BBD experimental domain

Coded variables	Real variables	Levels		
		-1	0	+1
X_1	U_1: current intensity, A	0.5	1.5	2.5
X_2	U_2: time, min	20	40	60
X_3	U_3: pH	4	7	10

With RSM, a collection of statistical tools is used to build mathematical models to evaluate the effects of several variables and search for the optimum conditions for specified responses [37]. The resulting mathematical models are generally second-degree polynomial functions (see Eq. (6))**:**

$$Y = b_0 + \sum b_i X_i + \sum\sum b_{ij} X_i X_j + \sum b_{ii} X_i^2 \; ; \; i \neq j \tag{6}$$

where Y, b_0, b_i, b_{ij}, b_{ii} and X_i or X_j represent the predicted response, the constant coefficient, the linear coefficient, the interaction coefficient, the quadratic coefficient and the coded values of the factors, respectively. The coefficients of the mathematical model were estimated using the less squares method [38]. The conversion of real values into coded values of factor i is done with Eq. (7):

$$X_i = (U_i - U_{i,0})/\Delta U_i \tag{7}$$

Where X_i, U_i, $U_{i,0}$ and ΔU_i represent coded value, real value, the real value in the centre of the experimental domain and the step of variation, respectively. Design Expert software was used for the calculation of the model coefficients and the coefficient of determination (R^2), the analysis of variance (ANOVA) with a confidence level of 95 % and to determine the optimal treatment conditions. For multiobjective optimization, acceptable compromises have been found with the desirability function approach [9].

Analytical details

Phosphate, nitrate, ammonium and nitrite concentrations were determined using a UV visible spectrophotometer (JASCO V-530 UV/VIS, Japan) according to AFNOR standards. The sludge obtained after filtration was dried in an oven at a temperature of 105 °C for 24 hours and then analysed by XRD and FTIR. XRD analysis was carried out with 2θ values between 10 and 70° using a diffractometer from Rigaku - Miniflex II, Japan. The identification of the functional groups on the surface of the sludge was possible through infrared spectral data obtained from the Perkin Elmer FTIR spectrometer (Spectrum BX). The samples were first conditioned as KBr pellets and scanned over the range 650 to 4000 cm^{-1}.

Economic aspect

For the evaluation of operating cost (OC, USD), the electrode material cost and electricity charges were taken into account [39] (Eq. (8)):

$$OC = a\text{ELC} + b\text{ENC} \tag{8}$$

where ELC (kg), ENC (kWh), *a* and *b* represent the electrode consumption, the energy consumption, the unit price of the energy estimated approximately at 0.059 USD/kWh and the unit price of aluminium estimated at 1.7618 USD kg^{-1}, respectively [9].

Electrode consumption is obtained by differentiating the electrode mass at the beginning and the end of each experiment. It can be expressed according to Faraday's law as:

$$ELC = ItM / nF \qquad\qquad (9)$$

where *I* / A, *t* / s, M / g mol^{-1} and *F* (96500 C mol^{-1}) represent the current intensity, the electrolysis time, the aluminium molecular weight and the Faraday's constant.

The energy consumption was estimated using Eq. (10):

$$ENC = UIt \qquad\qquad (10)$$

where *U* / V, *I* / A and *t* / h represent the cell voltage, the current intensity value and the electrolysis time, respectively.

Results and discussion

Development of quadratic models and analysis of variance (ANOVA)

The results of the tests carried out from the combination of the three independent variables according to the BBD are given in Table 3. With the three factors, fifteen (15) tests were carried out with Al electrodes.

According to Table 3, phosphate removal rates (Y_1) varied between 54.5 and 96 %, nitrate removal (Y_2) varied between 19.58 and 70.06 % and the amount of ammonium generated (Y_3) varied between 4.94 and 15.66 mg L^{-1}. The high removal rates of phosphate and nitrate do not correspond to the same experimental conditions. Current intensity of 1.5 A, a treatment time of 40 min and a pH 7 were necessary to eliminate 96 % of phosphate, whereas, with the nitrate, a current of 2.5 A, a duration of 60 min and a pH 7 were necessary. Also, the quantities of nitrite (0.156 to 0.368 mg L^{-1}) obtained are very low and even lower than the limit value authorized by the US EPA (3 mg L^{-1}) [40]. This low level confirms that nitrite is an intermediate product during the electro-reduction of nitrate. Regarding operating cost (Y_4), the values vary from 0.251 to 2.51 USD m^{-3}.

***Table 3.** Experience matrix and results of BBD*

Runs	Coded values			Responses				
	X_1	X_2	X_3	Y_1 / %	Y_2 / %	Y_3 / mg L^{-1}	Y_4 / USD m^{-3}	$C_{NO_2^-}$ / mg L^{-1}
1	-1	-1	0	54.5	19.58	4.94	0.251	0.156
2	1	-1	0	89.5	35.00	8.29	1.077	0.368
3	-1	1	0	82.0	36.77	12.30	0.710	0.353
4	1	1	0	89.0	70.06	15.66	3.640	0.350
5	-1	0	-1	82.0	38.33	10.44	0.540	0.182
6	1	0	-1	92.0	49.39	14.65	2.510	0.328
7	-1	0	1	64.0	31.96	10.04	0.506	0,326
8	1	0	1	94.0	45.19	14.61	2.170	0.39
9	0	-1	-1	87.5	17.77	6.08	0.700	0.273
10	0	1	-1	93.5	66.34	12.40	2.380	0.354
11	0	-1	1	60.5	18.37	5.43	0.660	0.280
12	0	1	1	91.0	49.15	11.35	2.280	0.368
13	0	0	0	96.0	39.02	11.01	1.516	0.307
14	0	0	0	91.0	40.61	11.78	1.507	0.327
15	0	0	0	96.0	44.94	10.87	1.418	0.312

Taking into account the variation of the responses according to the trials, the modelling of the responses by multiple regression allows having the following equations (Eqs. (11) to (13)):

Phosphate removal efficiency, %

$$Y_1 = 94.330 + 10.250X_1 + 7.940X_2 - 5.690X_3 - 7.850X_1^2 - 7.730X_2^2 - 3.480X_3^2 -$$
$$- 7.000X_1X_2 + 5.000X_1X_3 + 6.130X_2X_3 \tag{11}$$

Nitrate removal efficiency, %

$$Y_2 = 41.520 + 9.120X_1 + 16.450X_2 - 3.400X_3 + 1.070X_1^2 - 2.240X_2^2 - 1.380X_3^2 +$$
$$+ 4.470X_1X_2 + 0.543X_1X_3 - 4.450X_2X_3 \tag{12}$$

Ammonium generated, mg L^{-1}:

$$Y_2 = 11.220 + 1.940X_1 + 3.370X_2 - 0.267X_3 + 1.350X_1^2 - 2.270X_2^2 - 0.134X_3^2 +$$
$$+ 0.025X_1X_2 - 0.090X_1X_3 - 0.100X_2X_3 \tag{13}$$

Before the optimization step, it is important to check the quality of models through the analysis of variance (ANOVA). ANOVA analysis allows us to study the significance of the models and the lack of fit. The significance of the models is acquired for high Fischer values (*F*-values) and low probability values (*p*-value) less than 5 % [41]. The lack of fit of the models allows to assess the suitability of the models by comparing the residual error to the pure error from replication [42]. The statistical ANOVA based on the BBD was carried out with the Design Expert and summarised in Table 4.

Table 4. *ANOVA for fit of each response*

Responses	Sources	Squares sum	df*	Medium square	*F*-value	*p*-value, %
Y_1	Regression	2486.6	9	276.29	26.97	0.102
	Residual	51.23	5	10.25	-	-
	Lack of fit	34.56	3	11.52	1.38258	44.6
	Pure error	16.67	2	8.33	-	-
	Total	2537.83	14	-	-	-
	$R^2 = 0.9798$; $R^2_{adj.} = 0.9435$					
Y_2	Regression	3113.78	9	345.98	9.12	1.27
	Residual	189.65	5	37.93	-	-
	Lack of fit	170.87	3	56.96	6.07	14.5
	Pure error	18.77	2	9.39	-	-
	Total	3303.43	14	-	-	-
	$R^2 = 0.9426$; $R^2_{adj.} = 0.8393$					
Y_3	Regression	149.24	9	16.58	41.68	0.0358
	Residual	1.99	5	0.3979	-	-
	Lack of fit	1.51	3	0.5030	2.1	33.9
	Pure error	0.4808	2	0.2501	-	-
	Total	151.23	14	-	-	-
	$R^2 = 0.9868$; $R^2_{adj.} = 0.9632$					

*degree of freedom

According to this table, the *F*-values (26.97 for Y_1, 9.12 for Y_2 and 41.68 for Y_3) are above the critical value ($F_C = 4.77$) and *p*-values (0.102 % for Y_1, 1.27 % for Y_2 and 0.0358 % for Y_3) are below 5 %, showing that the models are statistically significant. The variations in predicted responses are, therefore, not random but are due to variations in the factors. The lack of fit of models is not significant as the p-values are high and above 5 % (44.6 % for Y_1, 14.5 % for Y_2 and 33.9 % for Y_3). The absence of the lack of fit shows that the adequacy of the generated models is verified [42]. Furthermore, the values of R^2 close to unity (0.9798, 0.9426 and 0.9868 for Y_1, Y_2 and Y_3, respectively), prove a strong fit between

the experimental and predicted responses. So, the models explain the electrocoagulation process well. Only 2.02, 5.74 and 1.32 % of the total variations could not be explained by the empirical models of phosphate removal rate, nitrate removal rate and generated ammonium, respectively.

Effect of independent variables on phosphate removal

Figure 2 shows the interaction terms of phosphate removal efficiency. Keeping pH at the centre of the experimental domain, Figure 2a shows the interactions between current intensity and electrolysis time. It appears that better phosphate removal rate of 96 % is recorded for high current intensity (2.5 A) and long processing times (60 minutes). Previous studies have demonstrated that increasing current intensity and electrolysis time positively affect EC phosphate removal [22]. In fact, an increase in the current intensity and the electrolysis time help to release large quantities of Al^{3+} ions, OH^- ions and hydrogen gas in aqueous medium according to Faraday's law [7]. These ions can precipitate directly phosphate as $AlPO_4$ or can form a large quantity of metal hydroxides $Al(OH)_3$, increasing the adsorption sites of phosphate [22]. Also, the large quantity of hydrogen gas could help to float phosphate out of the water [43]. The graph in Figure 2b shows the interaction between current intensity and pH on phosphate removal. It allows the detection of pH zones where the optimum is located. The graph shows that pH has a negative effect on phosphate removal. To achieve high phosphate removal efficiency, the pH must be at a low level. It is well known that pH is one of the key factors having a significant effect on the performance of the EC process because it affects the availability of the various coagulant forms in equilibrium in water as well as the surface charges of the coagulant species [44]. At pH values of 4-7, $Al(OH)_3$, having low solubility and apparent positive charges, can easily adsorb the predominant species of anionic phosphates ($H_2PO_4^-$, HPO_4^{2-}) by neutralization [25,45]. On the other hand, at pH greater than 10, $Al(OH)_3$ passes under the ionic form $Al(OH)_4^-$ thus losing its capacity for adsorbing phosphate anions due to the forces of electrostatic repulsion [45].
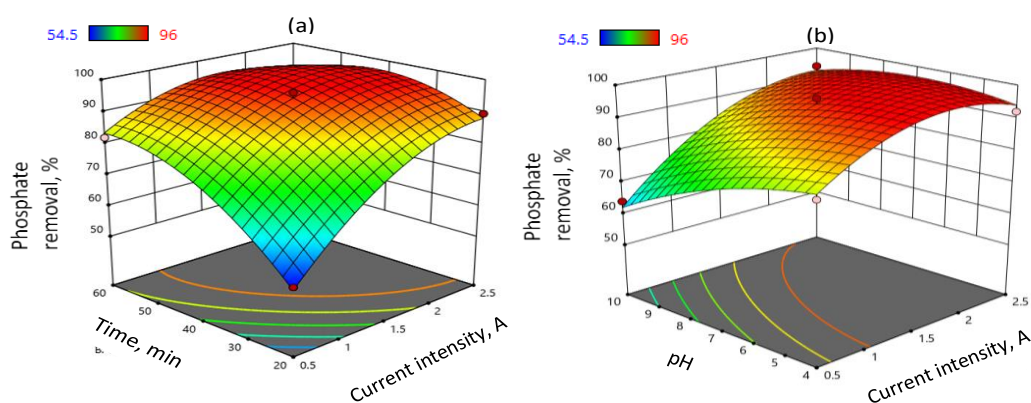

Figure 2. *3D response surface plots showing the evolution of phosphate removal for: (a) current intensity-time interaction (X_1X_2) and (b) current intensity-pH interaction (X_1X_3)*

Effect of independent variables on nitrogen compounds removal

The relationships between nitrate removal efficiency and the interaction terms are shown in Figure 3. According to Figure 3a, a high nitrate removal efficiency of 70 % is recorded for high current intensity (2.5 A) and long treatment time (60 minutes). Figure 3b shows that increasing in pH values has a negative effect on nitrate removal efficiency. The removal rate decreases from 55 % to approximately 27 % when the pH increases. The increase in nitrate removal rate with current (or time) can be explained by the large quantity of $Al(OH)_3$ produced by increasing nitrate adsorption sites [24,32,46]. Additionally, the oxidation rate of the anode increases with current intensity, resulting in a high

J. Ano *et al.*

J. Electrochem. Sci. Eng. **13(6)** (2023) 1081-1096

number of electrons at the interface electrodes/aqueous solution (Eq.(1)) that reduces electrochemical nitrate to ammonium, nitrite and nitrogen gas [32]**.** This is responsible for increasing the ammonium content in the medium (Figure 5a). A higher ammonium content occurred for high current intensity and long reaction time. 15.66 mg L^{-1} of ammonium are formed when current intensity and reaction time reach 2.5 A and 60 min, respectively. The effect of pH on nitrate removal could be due to the high availability of protons in an acid medium since the reduction of nitrate to ammonium consumes protons (Eqs. (14) and (15)) [9] :

$$NO_3^- + H_2O + 2e^- \rightarrow NO_2^- + 2OH^- \tag{14}$$

$$NO_3^- + 6H_2O + 8e^- \rightarrow NH_3 + 9OH^- \tag{15}$$

Indeed, by increasing pH of water, the number of protons decreases, resulting in the electrochemical reduction of nitrate. The improvement in the removal rate of nitrate at acidic pH can also be explained by the favourable adsorption of nitrate anion on the positive surface of $Al(OH)_3$ [47]. Finally, Figure 4b shows the insignificant effect of pH on ammonium generated.
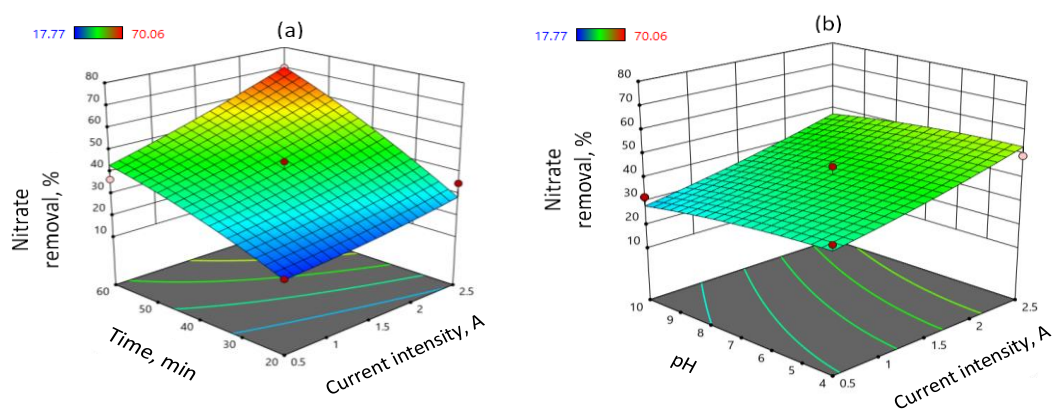

Figure 3. *3D response surface plots showing the evolution of nitrate removal for: (a) current intensity-time interaction (X_1X_2) and (b) current intensity-pH interaction (X_1X_3)*
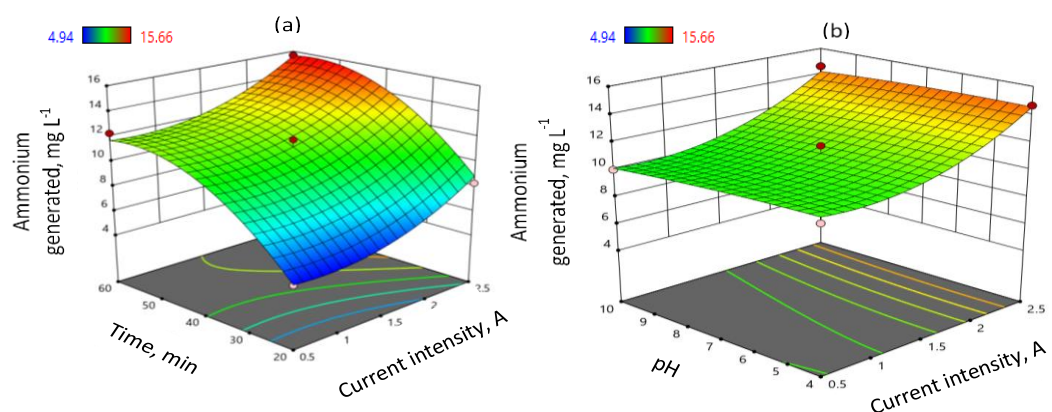

Figure 4. *3D response surface plots showing the evolution of ammonium generated: (a) current intensity-time interaction (X_1X_2) and (b) current intensity-pH interaction (X_1X_3)*

Process optimization and validation of optimal conditions

In this section, the optimal values of current intensity, electrolysis time and initial pH for the simultaneous phosphate and nitrate removals were studied. The objective is to maximize nutrient removal. The maximum overall desirability is 0.93 and the optimal conditions are defined by a current intensity of 2.45 A, an electrolysis time of 58 minutes and pH of 6.8. These conditions predict a phosphate removal rate of 91 %, a nitrate removal rate of 68 % and an amount of ammonium

generated of 15.22 mg L^{-1}. The validation tests were tripled and the experimental results are as follows: 89.21±3.36 % of phosphate removal; 69.06±1.84 % of nitrate removal; 3.35±0.08 USD m^{-3} of treatment cost; 13.68±1.92 mg L^{-1} of ammonium generated.

Unsurprisingly, these experimental results are strongly in agreement with the results predicted by the model. Consequently, the response surface methodology with a desirability approach has proven to be an effective method for optimizing the experimental conditions.

Application of the optimal condition on real domestic wastewater

The real domestic wastewater was treated, without the addition of electrolyte support, under optimum operating conditions of 2.45 A, 58 minutes treatment time and pH 6.8. Under these conditions, after 58 minutes of treatment, the residual concentrations of phosphate and nitrate are 7.03±0.54 and 11.68±1.02 mg L^{-1}, respectively. This corresponds to a phosphate removal efficiency of 93.0 % and a nitrate removal efficiency of 90.3 %. At the end of the treatment, a residual ammonium concentration of 30.9 mg L^{-1} and a treatment cost of 2.11 USD m^{-3} were recorded.

Electrooxidation of generated ammonium

The removal efficiency of phosphates and nitrates, as well as the emergence of by-products (ammonium and nitrite), were examined under optimal conditions by adding different amounts of NaCl electrolyte to the reactor (from 0 to 3 g) (Figure 5). According to Figure 5, nitrate removal rate decreases from 90.26 to 68.43 (Figure 5a). Regarding phosphate ions, the efficiency rate increases slightly and reaches the value of 94.72 % for sodium chloride mass of 1.5 g, then decreases until reaching a rate of 88.02 % (residual concentration of 11.98 mg L^{-1}). This residual phosphate content is below the discharge standard authorized in Ivory Coast. Figure 5b shows the evolution of nitrogen compounds in the aqueous medium. An increase in nitrate levels and a decrease in ammonium generated are observed.
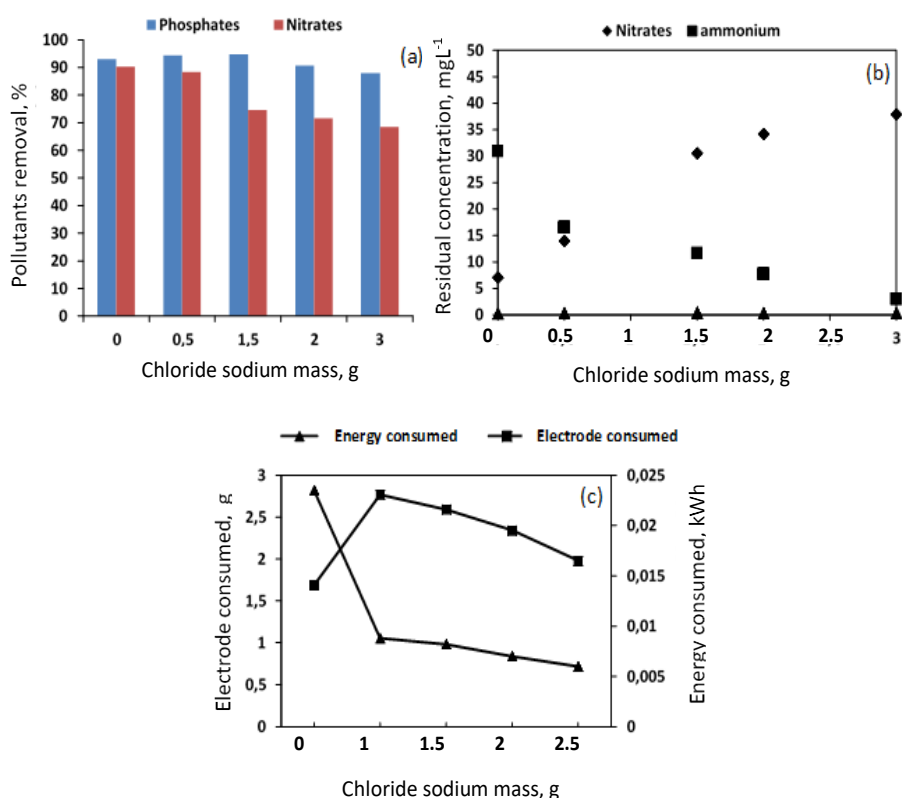

Figure 5. *Effect of NaCl dose on the removal of (a) phosphates and nitrates, (b) nitrogen compounds and (c) electrode and energy consumed*

The residual concentration of nitrate increases in the medium and reaches the content of 37.88 mg L^{-1}, while the ammonium decreases from 30.9 to 2.95 mg L^{-1}. Nitrate residual concentration is below the discharge standards (see Table 1). The evolutions of nitrate and ammonium levels is in agreement with previous work suggesting the existence of competition between chloride and nitrate at the interface of Al(OH)$_3$ adsorption sites [48]. In addition, the chloride ions present in the solution oxidize electrochemically into active chlorine in the form of hypochlorite (ClO$^-$) ions, which react with nitrite to regenerate nitrate (see eq. (16)). The decrease in ammonium concentration is explained by its transformation into N$_2$ by the action of hypochlorite ((Eq. (17)).

$$NO_2^- + ClO^- \rightarrow NO_3^- + Cl^- \qquad\qquad\qquad (16)$$

$$2NH_4^+ + 3HClO \rightarrow N_2 + 3H_2O + 5H^+ + 3Cl^- \qquad\qquad\qquad (17)$$

The decrease in nitrate reduction efficiency could also be explained by the conversion of chlorides to chlorine, which delays the oxidation of aluminum to Al^{3+} ions. In fact, it will have a few Al(OH)$_3$ flocs to adsorb the maximum amount of nitrate. Thus, in the case of this study, it is observed that the electrode mass loss decreases with increasing amounts of NaCl (see Figure 5c). In addition, a decrease in power consumption was also observed due to the increase in conductivity associated with the increasing addition of electrolytes. The higher the conductivity, the lower the voltage of the electrolytic cell, resulting in a reduction in energy consumption. This increase in conductivity is conducive to phosphate removal up to a mass of 1.5 g of electrolyte, followed by a slight decrease. This decrease in efficiency is due to the competition effect between the adsorption of phosphate and chloride ions on aluminum hydroxides.

Residues sludge characterization

The dried EC sludge, obtained under optimal conditions, was analysed by XRD and FTIR in order to identify the nature of the crystalline phases and the surface functional groups (Figure 6). To this end, the spectrum (Figure 6a) reveals the existence of distinct peaks that is attributed to Al(OH)$_3$ and AlPO$_4$ [32]. In addition, examination of IR spectrum (Figure 6b) made it possible to associate the characteristic peaks with the functional groups present on the sludge surface. It can be seen that the spectrum is characterized by a broad peak at about 3369 cm^{-1}. This peak is attributed to the -OH stretch in the Al(OH)$_3$ structure [49]. The peak at 1640 cm^{-1} is attributed to the bending of the hydroxyl groups of the water molecules [50]. Finally, the band observed around 1043.7 cm^{-1} is due to the bending vibration of Al-O-P in the phosphate ion [50]. The components of the precipitate are aluminum hydroxide, aluminum hydroxyphosphate and/or aluminum phosphates. The results of the FTIR spectra confirm that the phosphate is removed by adsorption, precipitation and co-precipitation.
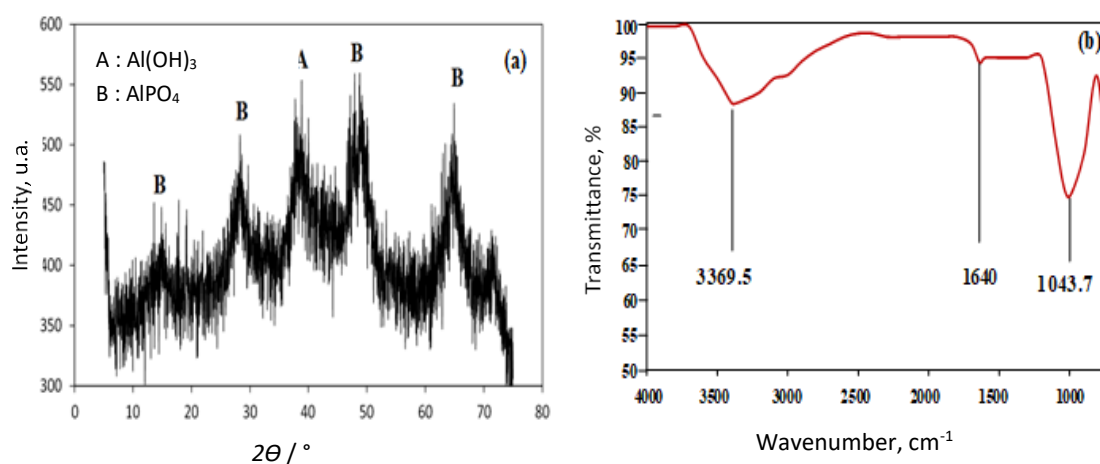

Figure 6. *XRD (a) and FTIR (b) spectrum of sludge*

From the XRD and FTIR spectra, nitrate was not detected in the crystalline phase of the dried sludge. However, to check for the presence of different nitrogen compounds, the sludge was dissolved in concentrated sulfuric acid. Then we added distilled water until we reached the volume of the reactor. The measurement of the levels of nitrogenous compounds reveals a content of 8.01 mg L^{-1} of nitrate, 3.02 mg L^{-1} of ammonium and 0.032 mg L^{-1} of nitrite. This result shows that part of the nitrate as well as these by-products, were trapped by the sludge produced during the treatment. Therefore, the analysis of the treated water and the sludge confirms that nitrate is eliminated by reduction to ammonium and adsorption.

Conclusion

The current study examined the potential of the EC process to simultaneously remove phosphate and nitrate from water as well as ammonium, which is the main by-product. This study also investigated the applicability of response surface methodology, in this case, the Box-Behnken design, to model and optimize the performance of simultaneous phosphate and nitrate removal. The factors taken into account are the current intensity, the initial pH and the treatment time. The results obtained indicate that the removal of phosphate and nitrate is more efficient at slightly acidic pH, at high current intensities and long treatment times. On the other hand, the removal of nitrate is accompanied by a significant production of ammonium. Multiobjective optimization of the EC process allowed the removal of 89.2 % of phosphate and 69.1 % of nitrate from synthetic water with 13.7 mg L^{-1} of ammonium generated and an operating cost of 3.35 USD m^{-3}. Then, 93.0 % phosphate and 90.3 % nitrate were recorded by applying the optimal conditions on real domestic effluent. Finally, the progressive addition of sodium chloride in the domestic effluent allowed the reduction of the remaining ammonium (30.9 mg L^{-1}) until reaching 2.95 mg L^{-1}. From the analysis of the sludge, the results revealed that phosphates were removed by adsorption on aluminum hydroxides and by precipitation as aluminum phosphate, while nitrates were removed by electroreduction to ammonium and by adsorption.

References

[1] P. M. Nyenje, J. W. Foppen, S. Uhlenbrook, R. Kulabako, A. Muwanga, Eutrophication and nutrient release in urban areas of sub-Saharan Africa — A review, *Science of The Total Environment* **408** (2010) 447-455. https://doi.org/10.1016/j.scitotenv.2009.10.020

[2] S. Wiriyathamcharoen, S. Sarkar, P. Jiemvarangkul, T. T. Nguyen, W. Klysuban, S. Padungthon, Synthesis optimization of hybrid anion exchanger containing triethylamine functional groups and hydrated Fe(III) oxide nanoparticles for simultaneous nitrate and phosphate removal, *Chemical Engineering Journal* **381** (2020) 122671. https://doi.org/10.1016/j.cej.2019.122671

[3] S. S. Lin, S. L. Shen, A. Zhou, H. M. Lyu, Assessment and management of lake eutrophication: A case study in Lake Erhai, China, *Science of The Total Environment* **751** (2020) 141618. https://doi.org/10.1016/j.scitotenv.2020.141618

[4] M. Velu, B. Balasubramanian, P. Velmurugan, H. Kamyab, A. V. Ravi, S. Chelliapan, C. T. Lee, J. Palaniyappan, Fabrication of nanocomposites mediated from aluminium nanoparticles/Moringa oleifera gum activated carbon for effective photocatalytic removal of

nitrate and phosphate in aqueous solution, *Journal of Cleaner Production* **281** (2020) 124553. https://doi.org/10.1016/j.jclepro.2020.124553

[5] H. Dong, C. S. Shepsko, M. German, A. K. Sengupta, Hybrid nitrate selective resin (NSR-NanoZr) for simultaneous selective removal of nitrate and phosphate (or fluoride) from impaired water sources, *Journal of Environmental Chemical Engineering* **8** (2020) 103846. https://doi.org/10.1016/j.jece.2020.103846

[6] I. A. Kumar, N. Viswanathan, Fabrication of zirconium (IV) cross-linked alginate/kaolin hybrid beads for nitrate and phosphate retention, *Arabian Journal of Chemistry* **13** (2020) 4111-4125. https://doi.org/10.1016/j.arabjc.2019.06.006

[7] M. Ghazouani, L. Bousselmi, H. Akrout, Combined electrocoagulation and electrochemical treatment on BDD electrodes for simultaneous removal of nitrates and phosphates, *Journal of Environmental Chemical Engineering* **8** (2020) 104509. https://doi.org/10.1016/j.jece.2020.104509

[8] J. Y. Park, Y. J. Yoo, Biological nitrate removal in industrial wastewater treatment: which electron donor we can choose, *Applied Microbiology and Biotechnology* **82** (2009) 415-429. https://doi.org/10.1007/s00253-008-1799-1

[9] J. Ano, B. G. H. Briton, K. E. Kouassi, K. Adouby, Nitrate removal by electrocoagulation process using experimental design methodology: A techno-economic optimization, *Journal of Environmental Chemical Engineering* **8** (2020) 104292. https://doi.org/10.1016/j.jece.2020.104292

[10] K. T. K. M. Prashantha, T. R. Mandlimath, P. Sangeetha, S. K. Revathi, S. K. Ashok Kumar, Nanoscale materials as sorbents for nitrate and phosphate removal from water, *Environmental Chemistry Letters* **16** (2018) 389-400. https://doi.org/10.1007/s10311-017-0682-7

[11] S. Pulkka, M. Martikainen, A. Bhatnagar, M. Sillanpää, Electrochemical methods for the removal of anionic contaminants from water - A review, *Separation and Purification Technology* **132** (2014) 252-271. https://doi.org/10.1016/j.seppur.2014.05.021

[12] D. Xu, Y. Li, L. Yin, Y. Ji, J. Niu, Y. Yu, Electrochemical removal of nitrate in industrial wastewater, *Frontiers of Environmental Science and Engineering* **12** (2018) 9. https://doi.org/10.1007/s11783-018-1033-z

[13] D. T. Moussa, M. H. El-Naas, M. Nasser, M. J. Al-Marri, A comprehensive review of electrocoagulation for water treatment: Potentials and challenges, *Journal of Environmental Management* **186** (2017) 24-41. https://doi.org/10.1016/j.jenvman.2016.10.032

[14] M. Alimohammadi, M. Askari, M. H. Dehghani, A. Dalvand, R. Saeedi, K. Yetilmezsoy, B. Heibati, G. McKay, Elimination of natural organic matter by electrocoagulation using bipolar and monopolar arrangements of iron and aluminum electrodes, *International Journal of Environmental Science and Technology* **14** (2017) 2125-2134. https://doi.org/10.1007/s13762-017-1402-3

[15] O. Dia, P. Drogui, G. Buelna, R. Dubé, Hybrid process, electrocoagulation-biofiltration for landfill leachate treatment, *Waste Management* **75** (2018) 391-399. https://doi.org/10.1016/j.wasman.2018.02.016

[16] S. Boinpally, A. Kolla, J. Kainthola, R. Kodali, J. Vemuri, A state-of-the-art review of the electrocoagulation technology for wastewater treatment, *Water Cycle* **4** (2023) 26-36. https://doi.org/10.1016/j.watcyc.2023.01.001

[17] A. Othmani, A. Kadier, R. Singh, C. A. Igwegbe, M. Bouzid, M. O. Aquatar, W.A. Khanday, M. E. Bote, F. Damiri, Ö. Gökkuş, F. Sher, A comprehensive review on green perspectives of electrocoagulation integrated with advanced processes for effective pollutants removal from water environment, *Environmental Research* **215** (2022) 114294. https://doi.org/10.1016/j.envres.2022.114294

[18] S. Manikandan, R. Saraswathi, Electrocoagulation technique for removing Organic and Inorganic pollutants (COD) from the various industrial effluents: An overview, *Environmental Engineering Research* **28** (2023) 220231. https://doi.org/10.4491/eer.2022.231

[19] H. Kamyab, M. A. Yuzir, N. Abdullah, L. M. Quan, F. A. Riyadi, R. Marzouki, Recent Applications of the Electrocoagulation Process on Agro-Based Industrial Wastewater: A Review, *Sustainability* **14** (2022) 1985. https://doi.org/10.3390/su14041985

[20] K. S. Hashim, R. Al Khaddar, N. Jasim, A. Shaw, D. Phipps, P. Kot, M. O. Pedrola, A. W. Alattabi, M. Abdulredha, R. Alawsh, Electrocoagulation as a green technology for phosphate removal from river water, *Separation and Purification Technology* **210** (2019) 135-144. https://doi.org/10.1016/j.seppur.2018.07.056

[21] M. Ebba, P. Asaithambi, E. Alemayehu, Development of electrocoagulation process for wastewater treatment: optimization by response surface methodology, *Heliyon* **8** (2022) e09383. https://doi.org/10.1016/j.heliyon.2022.e09383

[22] P. I. Omwene, M. Kobya, Treatment of domestic wastewater phosphate by electrocoagulation using Fe and Al electrodes: A comparative study, *Process Safety and Environmental Protection* **116** (2018) 34-51. https://doi.org/10.1016/j.psep.2018.01.005

[23] K. Govindan, M. Noel, R. Mohan, Removal of nitrate ion from water by electrochemical approaches, *Journal of Water Process Engineering* **6** (2015) 58-63. https://doi.org/10.1016/j.jwpe.2015.02.008

[24] T. Yehya, M. Chafi, W. Balla, C. Vial, A. Essadki, B. Gourich, Experimental analysis and modeling of denitrification using electrocoagulation process, *Separation and Purification Technology* **132** (2014) 644-654. https://doi.org/10.1016/j.seppur.2014.05.022

[25] J. Ano, A. S. Assémian, Y. A. Yobouet, K. Adouby, P. Drogui, Electrochemical removal of phosphate from synthetic effluent: A comparative study between iron and aluminum by using experimental design methodology, *Process Safety and Environmental Protection* **129** (2019) 184-195. https://doi.org/10.1016/j.psep.2019.07.003

[26] E. Karamati-Niaragh, M. R. A. Moghaddam, M. M. Emamjomeh, E. Nazlabadi, Evaluation of direct and alternating current on nitrate removal using a continuous electrocoagulation process: Economical and environmental approaches through RSM, *Journal of Environmental Management* **230** (2019) 245-254. https://doi.org/10.1016/j.jenvman.2018.09.091

[27] A. Dura, C. B. Breslin, Electrocoagulation using aluminium anodes activated with Mg, In and Zn alloying elements, *Journal of Hazardous Materials* **366** (2019) 39-45. https://doi.org/10.1016/j.jhazmat.2018.11.094

[28] A. Attour, N. B. Grich, M. M. Tlili, M. B. Amor, F. Lapicque, J.-P. Leclerc, Intensification of phosphate removal using electrocoagulation treatment by continuous pH adjustment and optimal electrode connection mode, *Desalination and Water Treatment* **57** (2016) 13255-13262. https://doi.org/10.1080/19443994.2015.1057537

[29] A. Attour, M. Touati, M. Tlili, M. B. Amor, F. Lapicque, J.-P. Leclerc, Influence of operating parameters on phosphate removal from water by electrocoagulation using aluminum electrodes, *Separation and Purification Technology* **123** (2014) 124-129. https://doi.org/10.1016/j.seppur.2013.12.030

[30] E. Karamati-Niaragh, M. R. A. Moghaddam, M. M. Emamjomeh, Techno-economical evaluation of nitrate removal using continuous flow electrocoagulation process: optimization by Taguchi model, *Water Supply* **17** (2017) 1703-1711. https://doi.org/10.2166/ws.2017.073

[31] K. S. Hashim, I. A. Idowu, N. Jasim, R. Al Khaddar, A. Shaw, D. Phipps, P. Kot, M. O. Pedrola, A. W. Alattabi, M. Abdulredha, R. Alwash, K. H. Teng, K. H. Joshi, M. H. Aljefery, Removal of phosphate from River water using a new baffle plates electrochemical reactor, *MethodsX* **5** (2018) 1413-1418. https://doi.org/10.1016/j.mex.2018.10.024

[32] M. Guo, L. Feng, Y. Liu, L. Zhang, Electrochemical simultaneous denitrification and removal of phosphorus from the effluent of a municipal wastewater treatment plant using cheap metal electrodes, *Environmental Science: Water Research and Technology* **6** (2020) 1095-1105. https://doi.org/10.1039/d0ew00049c

[33] A. Ziouvelou, A. G. Tekerlekopoulou, D. V. Vayenas, A hybrid system for groundwater denitrification using electrocoagulation and adsorption, *Journal of Environmental Management* **249** (2019) 109355. https://doi.org/10.1016/j.jenvman.2019.109355

[34] A. K. Benekos, M. Tsigara, S. Zacharakis, I. E. Triantaphyllidou, A. G. Tekerlekopoulou, A. Katsaounis, D.V. Vayenas, Combined electrocoagulation and electrochemical oxidation treatment for groundwater denitrification, *Journal of Environmental Management* **285** (2021) 112068. https://doi.org/10.1016/j.jenvman.2021.112068

[35] A. K. Benekos, F. E. Tziora, A. G. Tekerlekopoulou, S. Pavlou, Y. Qun, A. Katsaounis, D. V. Vayenas, Nitrate removal from groundwater using a batch and continuous flow hybrid Fe-electrocoagulation and electrooxidation system, *Journal of Environmental Management* **297** (2021) 113387. https://doi.org/10.1016/j.jenvman.2021.113387

[36] K. S. Hashim, A. H. Hussein, S. L. Zubaidi, P. Kot, L. Kraidi, R. Alkhaddar, A. Shaw, R. Alwash, Effect of initial pH value on the removal of reactive black dye from water by electrocoagulation (EC) method, *Journal of Physics: Conference Series* **1294** (2019) 072017. https://doi.org/10.1088/1742-6596/1294/7/072017

[37] S. L. C. Ferreira, V. A. Lemos, V. S. de Carvalho, E. G. P. da Silva, A. F. S. Queiroz, C. S. A. Felix, D. L. F. da Silva, G. B. Dourado, R. V. Oliveira, Multivariate optimization techniques in analytical chemistry - an overview, *Microchemical Journal* **140** (2018) 176-182. https://doi.org/10.1016/j.microc.2018.04.002

[38] B. G. H. Briton, L. Duclaux, Y. Richardson, K. B. Yao, L. Reinert, Y. Soneda, Optimization of total organic carbon removal of a real dyeing wastewater by heterogeneous Fenton using response surface methodology, *Desalination and Water Treatment* **136** (2018) 186-198. https://doi.org/10.5004/dwt.2018.22845

[39] L. S. Thakur, P. Mondal, Techno-economic evaluation of simultaneous arsenic and fluoride removal from synthetic groundwater by electrocoagulation process: optimization through response surface methodology, *Desalination and Water Treatment* **57** (2016) 28847-28863. https://doi.org/10.1080/19443994.2016.1186564

[40] E. Nazlabadi, M. R. A. Moghaddam, E. Karamati-Niaragh, Simultaneous removal of nitrate and nitrite using electrocoagulation/floatation (ECF): A new multi-response optimization approach, *Journal of Environmental Management* **250** (2019) 109489. https://doi.org/10.1016/j.jenvman.2019.109489

[41] N. Saigaa, S. Bouguessa, W. Boukhedena, M. Nacer, A. Nadji, A. Gouasmia, Optimization of the inhibition corrosion of carbon steel in an acidic medium by a novel eco-friendly inhibitor Asphodelus ramosus using response surface methodology, *Journal of Electrochemical Science and Engineering* **13** (2023) 469-490. https://doi.org/10.5599/jese.1628

[42] W. N. F. W. Hassan, M. A. Ismail, H. S. Lee, M. S. Meddah, J. K. Singh, M. W. Hussin, M. Ismail, Mixture optimization of high-strength blended concrete using central composite design, *Construction and Building Materials* **243** (2020) 118251. https://doi.org/10.1016/j.conbuildmat.2020.118251

[43] M. Majlesi, S. M. Mohseny, M. Sardar, S. Golmohammadi, A. Sheikhmohammadi, Improvement of aqueous nitrate removal by using continuous electrocoagulation/electroflotation unit with vertical monopolar electrodes, *Sustainable Environment Research* **26** (2016) 287-290. https://doi.org/10.1016/j.serj.2016.09.002

[44] S. Garcia-Segura, M. M. S. G. Eiband, J. V. de Melo, C. A. Martínez-Huitle, Electrocoagulation and advanced electrocoagulation processes: A general review about the fundamentals,

emerging applications and its association with other technologies, *Journal of Electroanalytical Chemistry* **801** (2017) 267-299. https://doi.org/10.1016/j.jelechem.2017.07.047

[45] V. Kuokkanen, T. Kuokkanen, J. Rämö, U. Lassi, J. Roininen, Removal of phosphate from wastewaters for further utilization using electrocoagulation with hybrid electrodes - Techno-economic studies, *Journal of Water Process Engineering* **8** (2015) e50-e57. https://doi.org/10.1016/j.jwpe.2014.11.008

[46] M. M. Emamjomeh, H. A. Jamali, M. Moradnia, Optimization of Nitrate Removal Efficiency and Energy Consumption Using a Batch Monopolar Electrocoagulation: Prediction by RSM Method, *Journal of Environmental Engineering* **143** (2017) 04017022. https://doi.org/10.1061/(ASCE)EE.1943-7870.0001210

[47] M. H. Abdel-Aziz, E. S. Z. El-Ashtoukhy, M. S. Zoromba, M. Bassyouni, G.H. Sedahmed, Removal of nitrates from water by electrocoagulation using a cell with horizontally oriented Al serpentine tube anode, *Journal of Industrial and Engineering Chemistry* **82** (2020) 105-112. https://doi.org/10.1016/j.jiec.2019.10.001

[48] M. Amarine, B. Lekhlif, M. Sinan, A. El Rharras, J. Echaabi, Treatment of nitrate-rich groundwater using electrocoagulation with aluminum anodes, *Groundwater for Sustainable Development* **11** (2020) 100371. https://doi.org/10.1016/j.gsd.2020.100371

[49] K. K. Garg, B. Prasad, Development of Box Behnken design for treatment of terephthalic acid wastewater by electrocoagulation process: Optimization of process and analysis of sludge, *Journal of Environmental Chemical Engineering* **4** (2016) 178-190. https://doi.org/10.1016/j.jece.2015.11.012

[50] D. Tibebe, Y. Kassa, A.N. Bhaskarwar, Treatment and characterization of phosphorus from synthetic wastewater using aluminum plate electrodes in the electrocoagulation process, *BMC Chemistry* **13** (2019) 107. https://doi.org/10.1186/s13065-019-0628-1